Performance Analysis of MPC Controller Applied for Hybrid PV-Wind Under Varying Weather Conditions

Houda LAABIDI[1,2], Houda JOUINI[2], and Abdelkader MAMI[2]

[1]ESPRIT School of Engineering Tunis, Tunisia
[2]UR-LAPER, Faculty of Sciences of Tunis, University of Tunis El Manar Tunis, Tunisia

Abstract: The studied system contains a photovoltaic conversion chain with a total power of 7.2 kW, a wind conversion chain (5.1 kW), two-level inverter related to the electrical grid through an RL filter. The control systems of the simulation model include the Model Predictive Controller (MPC), which is mainly applied for both DC/DC converters and three-phase inverter. The MPC strategy uses the mathematical model of the considered power converters in order to predict the possible future behaviors of the different controlled variables. It permits selecting the optimal voltage vector, which is able to ensure a minimization of the specified cost function. Modeling and simulation are achieved using PSIM software in order to verify the system's performances, highlighting many scenarios of varying meteorological conditions. The simulation responses prove that the proposed MPC algorithm can offer a fast transient response, an accurate reference tracking, a high-injected power quality with a low current THD (less than 1% in the steady state).

Keywords: Boost circuit; two-level inverter; Hybrid system; Model Predictive Control; THD

1. Introduction

Photovoltaic and Wind energies have considered the most promising energy solutions on a global scale. They have been strongly developed in recent years due to increasing electricity demand, rising oil prices and harmful environmental impacts caused by the non-renewable energy resources [1]. Especially, PV-wind power systems have improved their use in a hybrid configuration. The major key features of this hybrid renewable energy structure is to work in an isolated area or connected to the utility grid. This development is done through the growing interest of power electronic converters and renewable energy device's effectiveness. To ensure the world's energy needs, an increasing attention is being paid to the integration of renewable energy conversion systems into the electrical grid. These systems have led scientists and researchers to investigate several control strategies. The grid integration process introduced many issues such as power quality, efficiency, current waveforms and reliability. The PV-Wind hybrid system consists of DC/DC converters in order to extract the maximum power from the photovoltaic fields and the variable-speed wind turbines. The generated power from the hybrid system is fed into grid through a three-phase inverter by keeping average DC-link voltage as a fixed value. In literature, different PV-Wind hybrid system architectures have been studied and analyzed. In [2], a hybrid system combined of wind turbine, Solid Oxide Fuel Cell and battery is studied. Several DC/DC configurations are applied to connect all the renewable energy resources and storage devices to a common DC bus. The output of DC bus is injected to the grid via three-phase DC/AC converter in order to ensure the power procurement. In [3], the proposed hybrid power system consists of photovoltaic array, hydrogen technology and battery bank have been controlled using a management system. In [4], a grid connected Wind-PV hybrid system performances have been analyzed under grid perturbations such as polluted grid voltages, unbalanced grid voltages and the balanced voltage dip. [5] Presents the divers operating modes of a small hybrid AC/DC micro-grid in order to control the energy transmission between AC and DC bus. In addition to that, it guarantees a regulated system operation under different production and load conditions. [6] Discussed an isolated Hybrid PV-wind-diesel and battery storage system to supply a residential area or small business buildings. A Maximum power point tracking (MPPT) methods are estimated as one of the important parts in photovoltaic conversion chain

Received: August 16th, 2019. Accepted: November 9th, 2020
DOI: 10.15676/ijeei.2020.12.4.17

design to extract the optimum output power from a PV panel. Researchers have applied various MPPT techniques, Perturb and Observe (P&O) is commonly employed due to its lower cost and easy hardware implementation [7]. Incremental conductance ((InCond)) and hill climbing have been reviewed in [8]. The Optimized Steepest Gradient Method (OSGM) is an independent MPPT technique developed in [9], which is adopted in order to track the maximum power production by updating the photovoltaic voltage. The advantage of both MPPT algorithms is their simplicity of implementation. While the drawbacks of these methods are the high fluctuations that occur around the maximum power point (MPP), the system's inability to track the maximum power during rapidly climatic condition variations. [10] Depicts another MPPT method based on Fuzzy Logic (FL) that allows improving of MPPT algorithm performances in terms of low oscillations around of MPP. A modified gray wolf optimization (MGWO) is studied to enhance MPPT capability for PV in partial shade conditions as presented in [11]. The main issues of these techniques are the drift problem arises from the fact that the climatic condition is non-uniform and the implementation part are complex. Adding a model predictive controller to the conventional InCond algorithm has been reviewed, studied and applied in this work. The considered algorithm can offer several benefits such as: suitable performance for extraction correctly the maximum power under different irradiation levels and reduce oscillations around MPP.

Three-phase grid connected converters are mostly applied for a wide sector, such as electrical drive systems, loads fed through AC-DC converters and distributed power generations including renewable energy field. The grid-side inverter control is generally divided into three steps:

- The DC-link voltage control step: it is intended to determinate the direct-axis current trajectory using the conventional PI controller.
- Current control step: it is usually designed to control the injected current into the grid.
- The Phased Locked Loop (PLL) is a popular technique used for grid synchronization in order to estimate the phase angle of the grid voltage.

Recently, researchers have focused on the three-phase grid connected inverter control, especially the grid current control that is considered the major key tasks in the grid-connected systems part. In fact, several current control techniques have been investigated in the literature. The classical linear control methods based on proportional-integral (PI) was presented by [12], [13] and [14]. They show that the Voltage-Oriented Control (VOC) strategy is applied to the voltage source inverter (VSI) due to its simple structure with a constant frequency switching; but the most important issues are their significant dependence on system parameters change. Both [15] and [16] have focused on the non-linear hysteresis control of a grid-connected system. The Direct Power Control (DPC) employed in this study is consisting to select the inverter switching states from a switching table. This operation is based on the measured errors between the grid-transferred powers and their corresponding reference signals. However, the high current harmonic distortion caused by the switching frequency variation is the main problems with this method. Two studies given by [17] and [18] have shown two internal current loops, which use sliding mode controller (SMC) due to its robustness against parameters variation but the high current THD is the major drawbacks of this technique. Actually, the Model predictive control (MPC) is considered the most promising grid-inverter techniques [19], [20], [21], [22], [23] due to their high performances.

In this context, MPC technique is adopted to extract the maximum power from renewable resources and transfer a high-quality power into the grid under variable and transient meteorological conditions. The idea behind MPC is to minimize the error between the predicted variable behaviors and their desired values by optimizing the defined cost function. After that, MPC-based scheme allows to choose and employ the optimal voltage vector. A computer simulation is carried out using PSIM software to validate the proposed MPC algorithm performances.

Thus, this work is organized as follows; the PV-Wind system structure and its component modeling are introduced in the first step. Then, the DC/DC converter as well as the grid-connected converter controllers are illustrated. Simulation results and discussions are carried out in the last section in order to present the validity and the effectiveness of the proposed MPC algorithm.

2. The proposed hybrid PV-Wind configuration

Figure 1 presents the proposed grid-connected hybrid PV-Wind power system. Two parallel PV-wind chains are linked via common DC bus. The first one contains a PV panel as DC power source related to DC/DC converter structure. While the second power block includes the wind turbine with its Permanent Magnet Synchronous Generator (PMSG) associated to uncontrolled rectifier and boost circuit. The maximum power extracted from these blocks is transferred to the utility grid through three phase inverter and RL filter. The proposed MPC algorithm controls all these used electronic converters in order to inject a high-quality power into the grid.

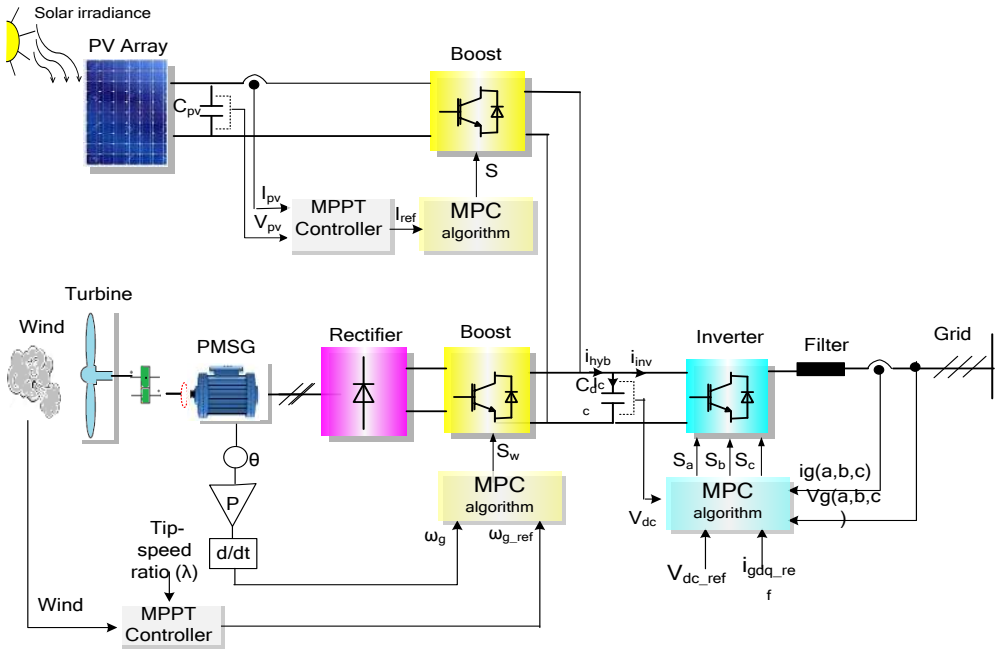

Figure 1. Photovoltaic-wind hybrid system configuration

3. Photovoltaic chain modelling

A. Photovoltaic Generator model

According to the photoelectric effect, the solar cell is able to transform directly the sun's radiation into electricity. These cells are associated in series or in parallel to form a solar panel. Various equivalent electric models of a solar cell are available in the literature. Figure 2 presents a basic circuit comprising a single-diode, which is applied to generate the current-voltage curves of the PV cell, a current source that is proportional to solar irradiation, a parallel resistance R_p and series resistance R_s [24].

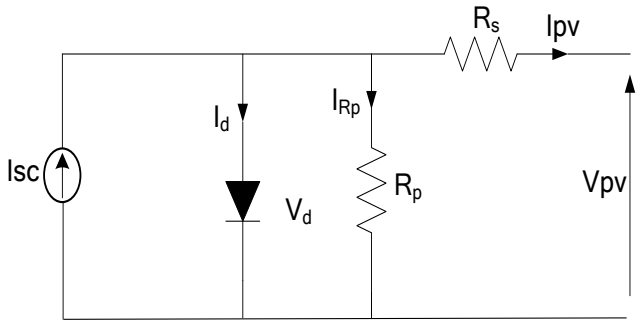

Figure 2. Photovoltaic cell model

The output current is represented by the following equations:

$$Ipv = I_{sc} - I_d - \frac{V_d}{R_p} \quad (1)$$

$$I_d = I_S\left(e^{\frac{V_d}{V_t}} - 1\right) \quad (2)$$

$$V_t = \frac{nKT}{q} \quad (3)$$

$$V_d = Vpv + Ipv.R_S \quad (4)$$

Where q is the elementary electron charge, k is the Boltzmann constant, T is the operating temperature in Kelvin, I_S is the diode saturation current (A) and n is the diode factor.

B. MPPT Controller based on InCond-MPC algorithm

A boost structure is adopted as a DC/DC converter to extract the maximum power available from the PV array. As depicted in Figure 3, the Incremental Conductance (InCond) MPPT method is required in order to determinate the reference current I_{ref} for the MPC scheme. The boost circuit is defined by two operation modes; during the first interval, when the switch s_{pv} is closed (s_{pv}=1), the diode is turned off. Therefore, the inductor starts to charge as illustrated in Figure 4 (a), the characteristic equations of this boost converter can be written as follows:

$$(s_{pv} = 1) \qquad \frac{dIpv}{dt} = \frac{Vpv}{L_{pv}} \quad (5)$$

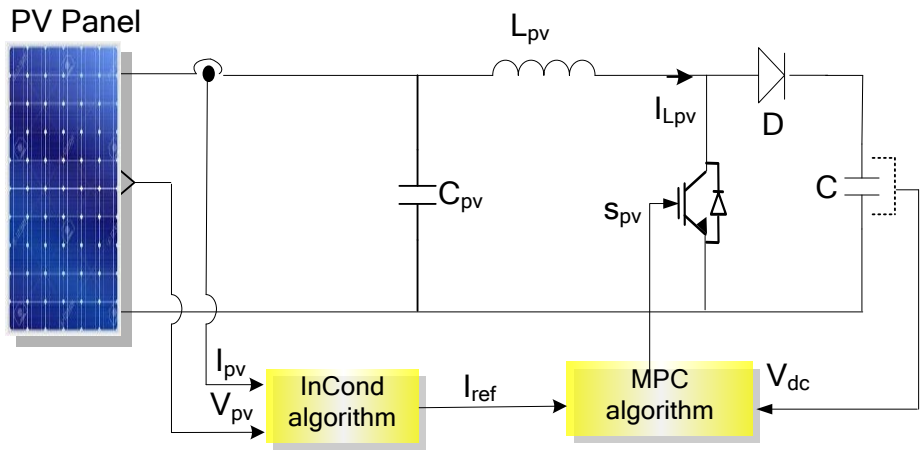

Figure 3. Photovoltaic boost controlled by InCond-MPC algorithm

The second operation modes occur when the power switch is opened (s_{pv}=0) and the diode is turned on as shown on Fig 4(b) [25], [26]. The corresponding equation can be written as follows:

$$(s_{pv}=0) \quad \frac{dIpv}{dt} = \frac{Vpv - V_{dc}}{L_{pv}} \tag{6}$$

With Vdc is the DC-link voltage.

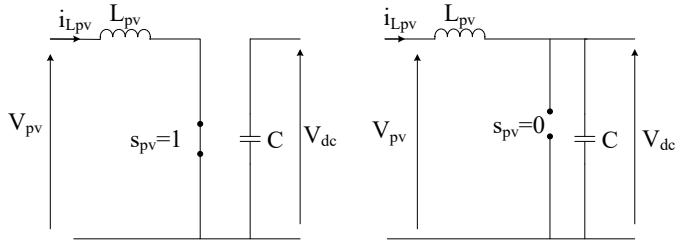

(a) (b)

Figure 4. Boost equivalent electrical circuits

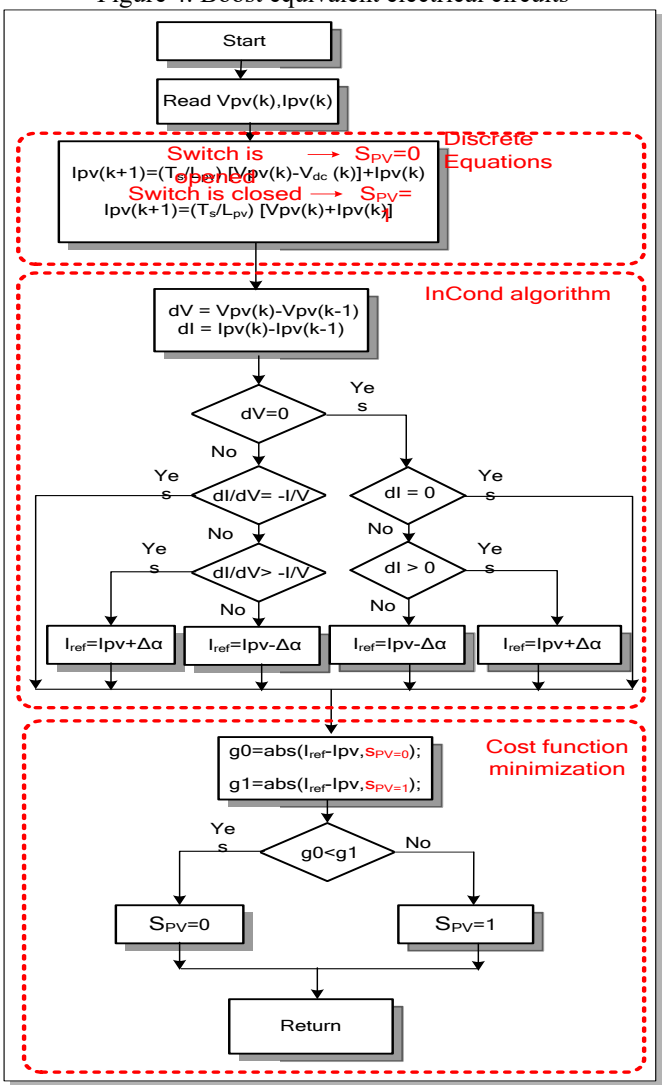

Figure 5. InCond-MPC algorithm Flowchart

Forward Euler equation as expressed by (7) is required to get a discrete-time model of the photovoltaic current behavior at sampling instant (k+1) as is written in (8) and (9):

$$\dot{x} \approx \frac{x(k+1)-x(k)}{T_s} \tag{7}$$

T_s is a sampling time

$$Ipv_{(s_{pv}=1)}(k+1) = Ipv(k) + \frac{Ts}{L_{pv}} Vpv \tag{8}$$

$$Ipv_{(s_{pv}=0)}(k+1) = Ipv(k) + \frac{Ts}{L_{pv}} (Vpv - V_{dc}) \tag{9}$$

The key feature of this MPC algorithm consists to forecast the future behavior of the desired control variables basing on the discrete time model representations. It predicts the next sampling period error between the predicted photovoltaic current and its reference value according to the predefined cost function optimization. The considered cost functions g0 and g1 will be obtained for both switching states and choose the optimal one that guarantees the nearest predicted value to the desired current trajectory as illustrated in Figure 5.

4. Wind energy chain modelling

A. Wind turbine modelling

The captured power by the variable-speed wind turbine can be written by:

$$P_t = \frac{1}{2}.\rho.\pi.{R_t}^2 C_p {V_w}^3 \tag{10}$$

Where V_w is the wind velocity, ρ is the air density, R_t is the wind turbine rotor radius (m), C_p is the power coefficient of the wind turbine, and λ is the tip-speed ratio is defined as [27] [28]:

$$\lambda = \frac{\omega_g .R_t}{V_w} \tag{11}$$

Where ω_g is the mechanical rotor speed (rad/s). This angular speed must be controlled to maintain λ at the optimum value (λ_{opt}) and then maximize the power coefficient as C_{pmax}. The produced wind turbine torque is calculated by the following equation:

$$T_m = \frac{P_t}{\omega_g} = C_p.\frac{\rho.S.{V_w}^3}{2}.\frac{1}{\omega_g} \tag{12}$$

B. Permanent Magnet Synchronous Generator (PMSG)

According to the synchronous (d,q) reference frame, the general PMSG model can be developed by the following equations [29] :

$$\begin{cases} \frac{di_d}{dt} = -\frac{R_s}{L_d}.i_d + \frac{\omega_e .L_q}{L_d}.i_q + \frac{V_d}{L_d} \\ \frac{di_q}{dt} = -\frac{R_s}{L_q}.i_q - \frac{\omega_e .L_d}{L_q}.i_d - \frac{\omega_e .\phi_f}{L_q} + \frac{V_q}{L_q} \end{cases} \tag{13}$$

Where i_d and i_q are d-q axis components of the stator current; V_d and V_q are d-q axis components of the stator phase voltage in the dq synchrounous reference frame; R_s is the stator resistance; L_d and L_q are d-q axis synchronous inductances ; ϕ_f is the permanent magnetic flux ; ω_e is the electrical rotor speed which depends on the mechanical speed ω_g ($\omega_e = p\omega_g$) with p is a pole pair number. The active and reactive powers are given by:

$$\begin{cases} P = \frac{3}{2}\left(V_d.i_d + V_q.i_q\right) \\ Q = \frac{3}{2}\left(V_q.i_d - V_d.i_q\right) \end{cases} \tag{14}$$

The mechanical equation is expressed as follows:

$$T_m - T_{em} = J.\frac{d\omega_g}{dt} + f.\omega_g \tag{15}$$

Where T_{em} is the electromagnetic torque applied to the PMSG rotor; f is the friction coefficient and J is the moment of inertia.

The PMSG electromagnetic torque is determined by:

$$T_{em} = \frac{3}{2}.p.\phi_f.i_q \quad (16)$$

C. Boost circuit controller

The chopper structure has two switching state operating modes, when the switch S is on (s_w=1), the second switching state when the switch is twisted off (s_w=0). The corresponding equations can be written as follows:

Closed switch (s_w=1):

$$\frac{di_L}{dt} = \frac{V_{in}}{L} \quad (17)$$

Opened switch (s_w=0):

$$\frac{di_L}{dt} = \frac{V_{in}-V_{dc}}{L} \quad (18)$$

Where i_L, V_{in}, V_{dc} and L are, respectively, the inductor current, the input converter voltage, the DC-link voltage and the boost inductance. The Model Predictive Control (MPC) block inputs are the calculated reference current i_{L_ref}, the measured inductor current i_L as well as the actual voltages (V_{in}) and (V_{dc}). The MPC block is divided into two steps, the predicted control variable calculations and the cost function optimization. A discrete-time equation for the future predicted inductor current at sampling instant (k+1) as shown in (19) and (20):

k is the current sampling instant and T_s is the sampling time.

$$i_{L(s_w=1)}(k+1) = i_L(k) + \frac{Ts}{L}V_{in} \quad (19)$$

$$i_{L(s_w=0)}(k+1) = i_L(k) + \frac{Ts}{L}(V_{in} - V_{dc}) \quad (20)$$

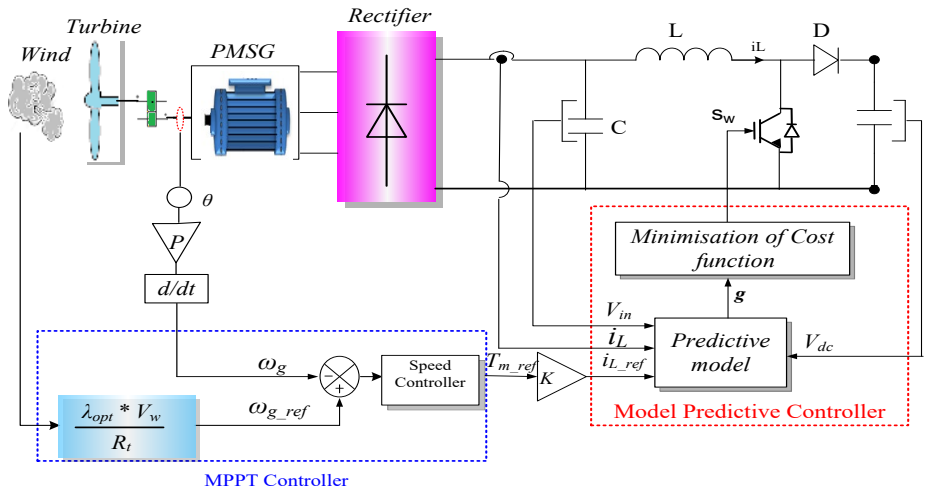

Figure 6. Wind DC/DC converter control

In this part, the defined cost functions g0 and g1 represent the optimized errors between the currents and their reference value as shown by:

$$g0 = \text{abs}(i_{L\_ref} - i_L(k+1), s_w=0) \quad (21)$$

$$g1 = \text{abs}(i_{L\_ref} - i_L(k+1), s_w=1) \quad (22)$$

The MPC scheme is given by Figure 6, the cost function is determined for both sampling switches, it ensures an accurate tracking of the measured inductor current i_L to its desired current trajectory i_{L_ref} controlled by the proposed method based on an MPC algorithm (Figure 7).

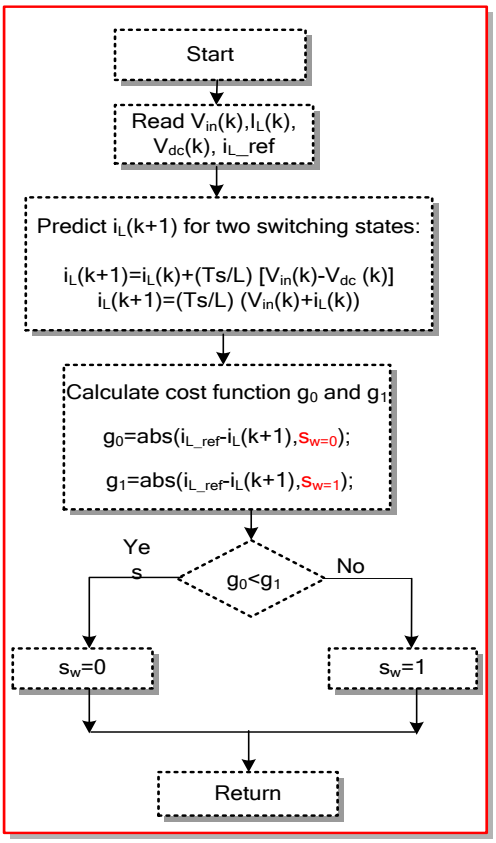

Figure 7. MPC-algorithm Flowchart

5. Grid side inverter controller

The MPC algorithm applied for two-level grid-connected inverter is described in Figure 8. As illustrated in this configuration, two cascade control loops are intended: the outer-voltage control loop and the inner-current control loop. Initially, the outer-voltage loop based on the linear PI-controller is applied to regulate the DC-link voltage V_{dc}. After that, the MPC based internal loop is designed in order to control the three-phase grid currents.

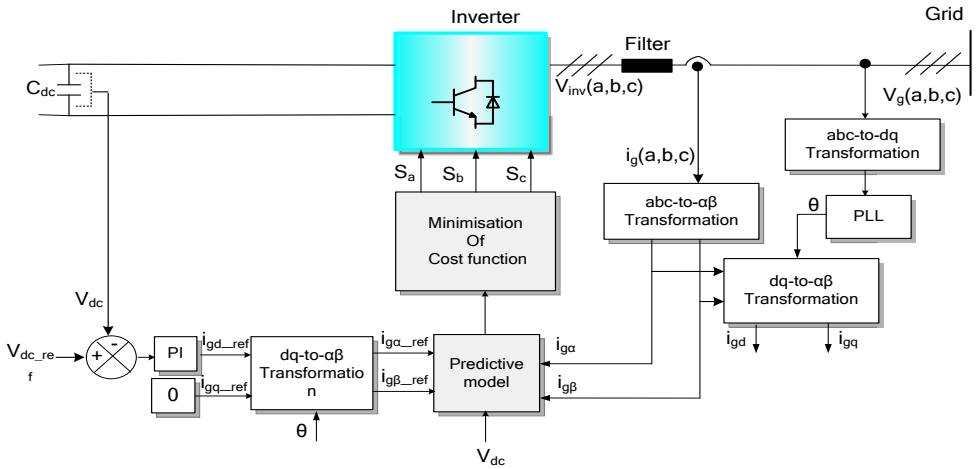

Figure 8. Grid inverter controlled by MPC

A. DC-link voltage control loop

To control the external loop, the DC-link voltage reference (V_{dc_ref}) is compared with the measured DC voltage (V_{dc}) and the error signal is fed to a PI controller (with proportional gain $G_{i(dc)}$ and integral time constant $\tau_{i(dc)}$) as shown in Figure 9.

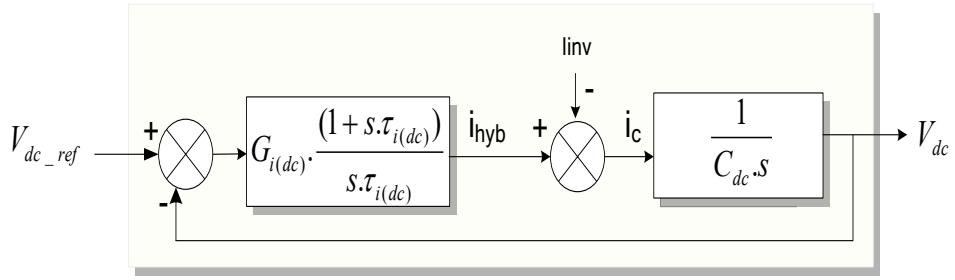

Figure 9. DC-link voltage loop

By neglecting I_{inv} current effect, the closed-loop transfer function is given by the following relation:

$$FTBF_{dc}(s) = \frac{V_{dc}}{V_{dc\_ref}} = \frac{(1+s.\tau_{i(dc)})}{\frac{\tau_{i(dc)}.C_{dc}}{G_{i(dc)}}.s^2+\tau_{i(dc)}.s+1} \quad (23)$$

We can deduce the PI controller parameters by choosing the desired damping ratio $\zeta_{(dc)}$ and the natural oscillation frequency $\omega_{n(dc)}$.

$$G_{i(dc)} = 2.\zeta_{(dc)}.C_{dc}.\omega_{n(dc)}) \quad (24)$$

$$\tau_{i(dc)} = \frac{2.\zeta_{(dc)}}{\omega_{n(dc)}} \quad (25)$$

B. Grid current controller

The MPC scheme applied for three-phase two-level power inverter uses the mathematical model in order to predict future behaviors of the controlled converter outputs for possible switching states. Then the optimal switching sequence that minimizes the predefined cost function is selected. This cost function is defined as a sum of the absolute values of the controlled variable errors. Thus, in each sampling period, the MPC controller ensures a minimal error between the considered variables and their desired values. Therefore, the desired current components $i_{g\alpha\_ref}$ and $i_{g\beta\_ref}$ are obtained through the application of the αβ transformation block. The three-phase grid currents (i_{ga}, i_{gb}, i_{gc}) are also transformed into $i_{g\alpha}$ and $i_{g\beta}$ components by applying Clarke Transformation.

$$i_{g\alpha} = \frac{2}{3}(i_{ga} - 0.5i_{gb} - 0.5i_{gc}) \quad (26)$$

$$i_{g\beta} = \frac{2}{3}(0.5\sqrt{3}i_{gb} - 0.5\sqrt{3}i_{gc} \quad (27)$$

The predictive process outputs are the future grid current behaviors $i^j_{g\alpha}(k+1)$ and $i^j_{g\beta}(k+1)$ at the (k+1) sampling time, which obtained by using Euler-forward equation [30].

$$i^j_{g\alpha}(k+1) = \left(1 - T_s\frac{R_f}{L_f}\right) i_{g\alpha}(k) + \frac{T_s}{L_f}(V^j_{inv\alpha} - V_{g\alpha}) \text{ with } (j = 0 \dots 7) \quad (28)$$

$$i^j_{g\beta}(k+1) = \left(1 - T_s\frac{R_f}{L_f}\right) i_{g\beta}(k) + \frac{T_s}{L_f}(V^j_{inv\beta} - V_{g\beta}) \text{ with } (j = 0 \dots 7) \quad (29)$$

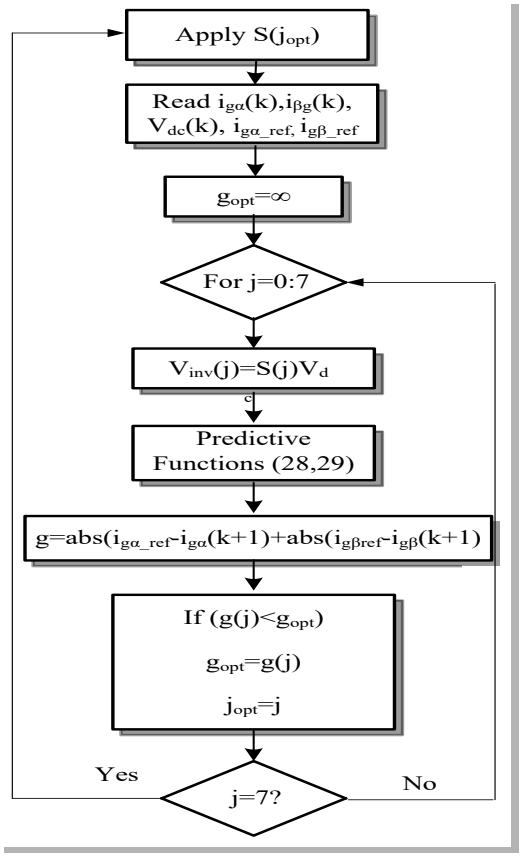

Figure 10. Flow diagram of MPC-based algorithm

Where ($V_{\text{inv}\alpha}^{j}, V_{inv\beta}^{j}$) are the space vector voltage of inverter, ($V_{g\alpha}, V_{g\beta}$) are the grid vector voltage. The predicted currents and their references are compared via a cost function as written in equation (30). The optimal voltage vector which ensures the predefined cost function optimization is chosen and the appropriate switching signals (S_a, S_b, S_c) are employed in the next sampling time.

$$g = \left|i_{g\alpha\_ref} - i_{g\alpha}^{j}(k+1)\right| + \left|i_{g\beta\_ref} - i_{g\beta}^{j}(k+1)\right| \quad (30)$$

Table 1. Inverter switching states and their voltage vectors

$V_{inv}{}^{j}$ ($S_aS_bS_c$)	$V_{inv\alpha}^{j}$	$V_{inv\beta}^{j}$
V_0(0 0 0)	0	0
V_1(1 0 0)	$2/3V_{dc}$	0
V_2(1 1 0)	$1/3V_{dc}$	$1/\sqrt{3}V_{dc}$
V_3(0 1 0)	$-1/3V_{dc}$	$1/\sqrt{3}V_{dc}$
V_4(0 1 1)	$-2/3V_{dc}$	0
V_5(0 0 1)	$-1/3V_{dc}$	$-1/\sqrt{3}V_{dc}$
V_6(1 0 1)	$1/3V_{dc}$	$-1/\sqrt{3}V_{dc}$
V_7(1 1 1)	0	0

The proposed MPC concept is based on eight possible different switching voltage vectors of the grid-connected inverter, as illustrated in Table. 1. Two combinations of them behave as zero

voltage vectors, and six others present two values, which are either positive or negative V_{dc}. So, only 7 switching possibilities are considered.

The predictive function g is required in order to select an optimal switching state that make the predicted grid current behaviors at next period close to their reference trajectories as shown in Figure 10.

6. Simulation results

The proposed MPC scheme performances for grid connected PV-wind hybrid system is demonstrated by means of computer simulation using PSIM package. The various parameters considered for simulation tests, are listed in Table 2.

Table 2. Parameters of PV-Wind hybrid system

Grid side converter parameters	
DC-link voltage V_{dc}	750 V
DC-link capacitor C	2000 µF
Filter resistance R_f	0.3 Ω
Filter inductance L_f	5mH
Grid frequency	50H

Photovoltaic module parameters	
Maximum power rating P_{mpp}	200W
Maximum Power Point Voltage V_{mpp}	26.3V
Maximum Power Point Current I_{mpp}	7.61A
Open Circuit Voltage Voc	32.9V
Short Circuit Current Isc	8.21A

Wind turbine parameters	
Nominal Output Power P_t	5.1 KW
Blade radius R_t	1.8m
Rated Wind Speed V_w	12m/s
Air Density ρ	1.22 kg/m3
Optimal tip speed ratio λ_{opt}	8.1
PMSG parameters	
Pole pairs number P	5
Stator resistance R_s	0.425Ω
D-axis inductance L_d	8.35 mH
Q-axis inductance L_q	8.35 mH
Moment of inertia J	0.01197 kg. m^2
Flux linkage Φ	0.433Wb

A. Case 1: The photovoltaic chain response

In this part, the PV array performances are studied during solar irradiance variation. While the temperature T is kept constant at 25°C during the overall simulation period. Figure 11 (a) illustrates the different solar irradiance levels. The proposed PV chain structure is fed through 36 PV panels arranged as twelve panels in series and three lines in parallel with a total power of 7.2 kW. As presented in the Figure 11(b), the proposed InCond-MPC algorithm ensure a setting time around 0.003s in order to reach the maximum PV power (3.1kW) according of solar irradiance variation, which is firstly equal to 400 W/m2. At 0.25 s the solar irradiance increases to the 650 W/m^2 and the output PV power is about 5 kW. After 0.5s the solar irradiance changes

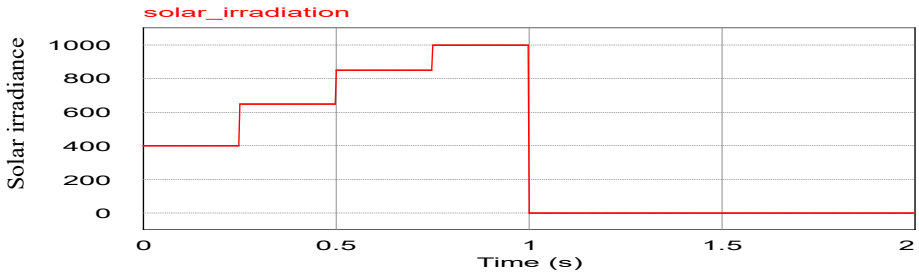

(a). Solar irradiance profile

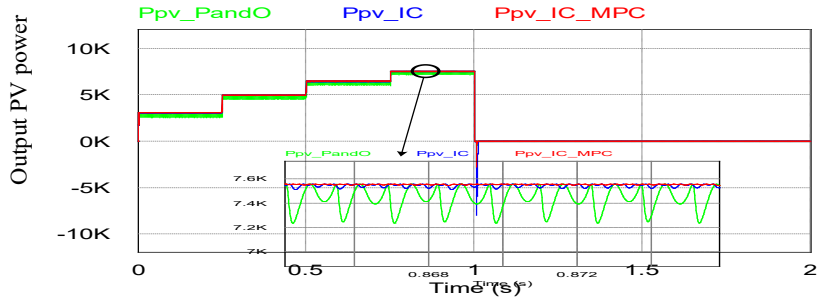

(b). Output PV power

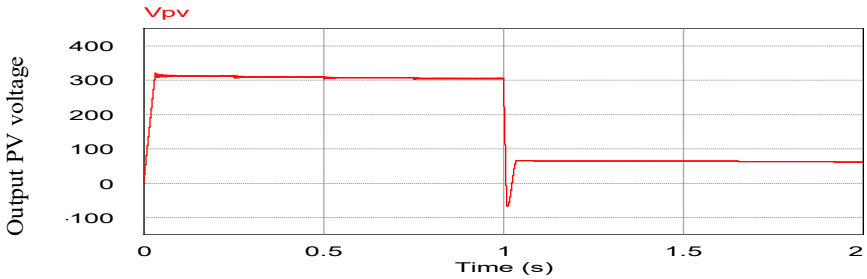

(c). Output PV voltage

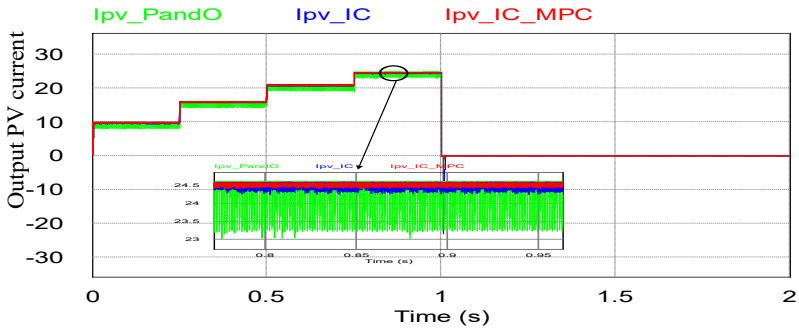

(d). Output PV current

Figure 11. PV system performances under varying solar irradiance

to 850 W/m^2 and the produced PV power is equal to 6.46 kW. It can be also seen that the PV array is able to deliver a maximum power of 7.2kW at 1000W/m^2. Figure 11 (c) depicts that the PV array voltage successfully tracks the voltage at maximum power (Vpv=315V) in order to

extract the maximum power from PV array under the solar irradiance change. Figure 11 (d) indicates that the output current from PV array is highly dependent on solar irradiance variations. When the solar irradiance is increased from 400 W/m^2 to 1000 W/m^2. The MPPT controller based on MPC algorithm respectively increases the I_{pv} array current from (9.8A) to (24.5A) to reach the maximum power from the PV array. Compared to other popular MPPT methods (P&O and InCond). Curves of green, blue and red colors are selected to show the response of P&O, InCond and InCond-MPC algorithms. The simulation test with the same PV array parameters is revealed that the proposed InCond-MPC algorithm presents an accurate tracking performance, a minimum oscillation around MPP and the ability to reach MPP due to its simple design.

B. Case 2: The wind chain response

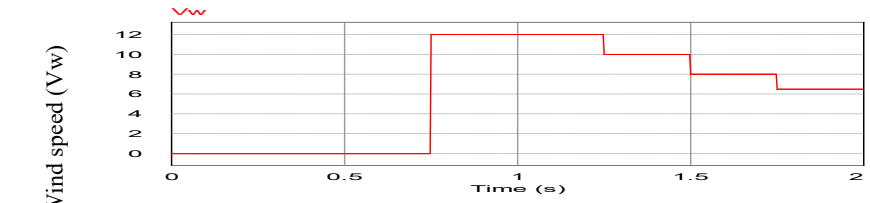

(a). Wind speed profile

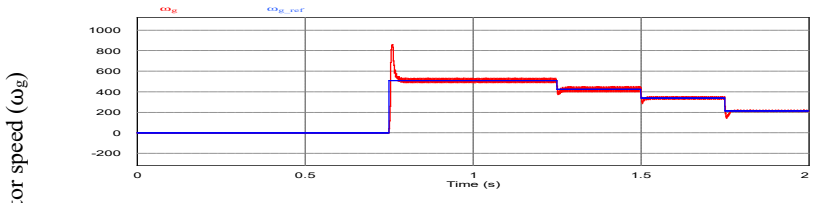

(b). Rotor speed and its reference

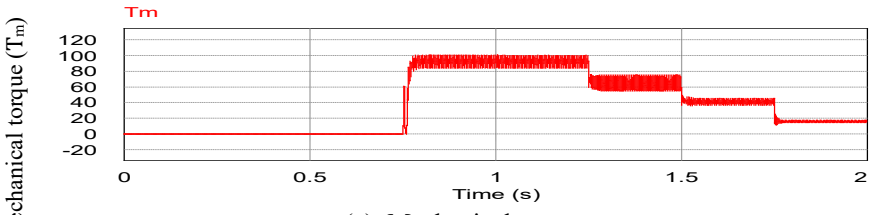

(c). Mechanical torque

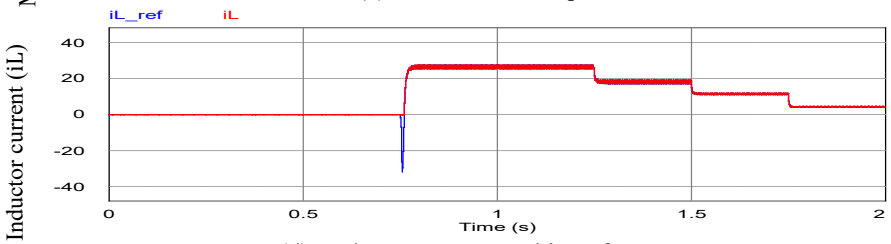

(d). Inductor current and its reference

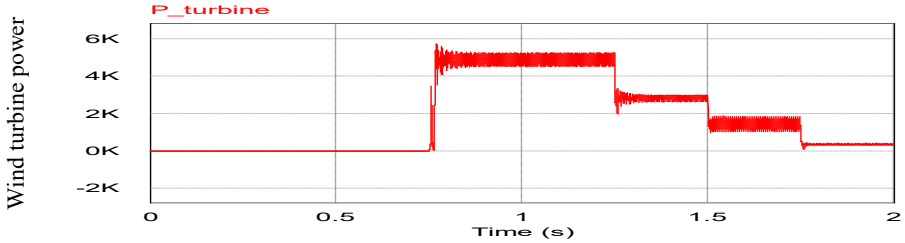

(e). Output wind turbine power

Figure 12. Wind system performances under wind speed variations

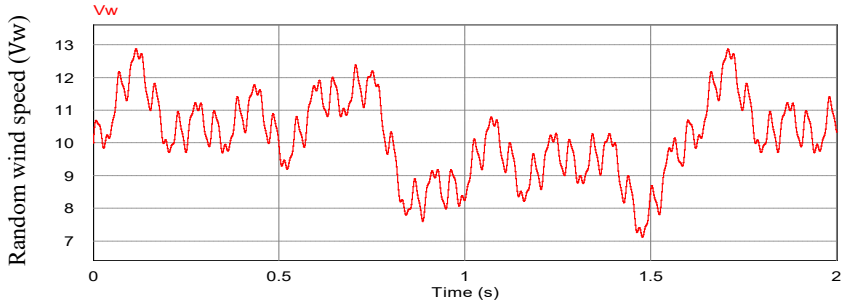

(a). Random wind speed profile

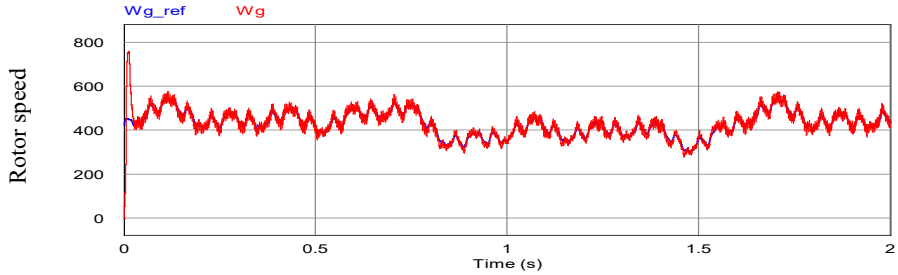

(b). Rotor speed and its reference

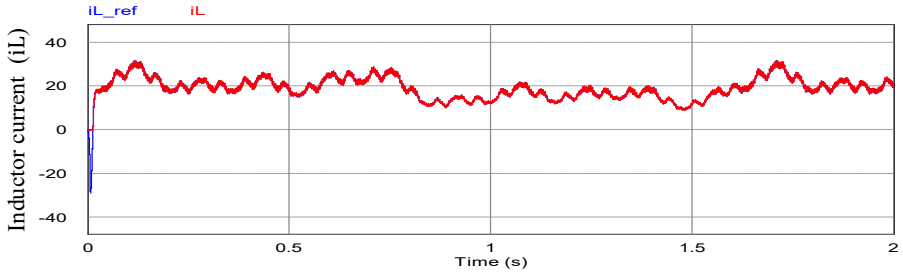

(c). Inductor current and its reference

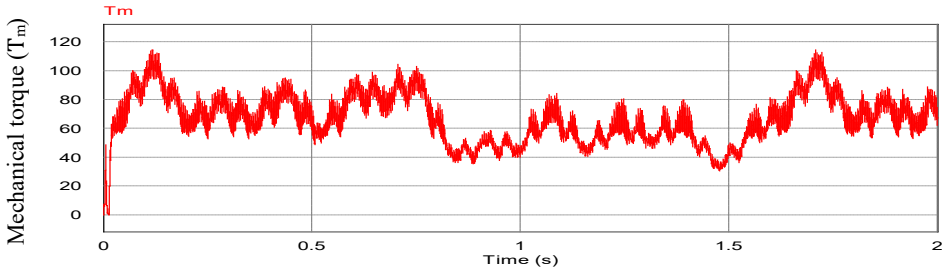

(d). PMSG mechanical torque

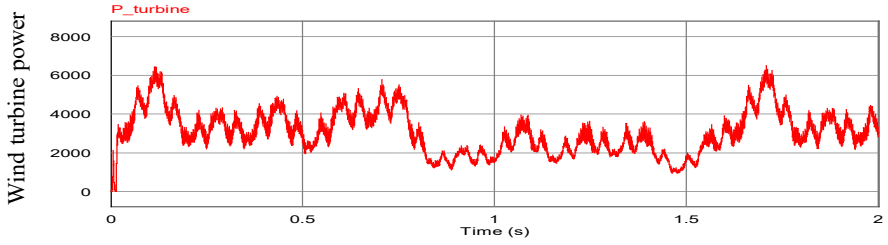

(e). Wind turbine power

Figure 13. Wind system performances under under random wind speed profile

In this subsection, the wind-chain performances corresponding to a linear wind speed profile is discussed. Figure 12 (a) presents the different wind speed levels. The wind speed decreases from 12 m/s to 5 m/s during the period from t=0.75 s to t=2 s. Figure 12 (b) depicts that the mechanical rotor speed ω_g reflects the variation of wind speed profile. It can be observed that an excellent rotor speed tracking to its reference trajectory ω_{g_ref} is appeared using a linear PI controller. As shown in the Figure 12 (c), the mechanical torque drops from 92.5 N.m to 16 N.m in response to the wind speed varies from 12 m/s to 5 m/s in order to extract the maximum power from a variable-speed wind turbine. It can be also seen in the Figure 12 (d) that the inductor current presents an accurate and a good following to its reference current under wind speed levels. At the initial condition, the wind conversion chain generates a maximum wind power equal to 5 kW according to the rated wind speed profile (12m/s). At 1.25 s the wind speed drops to 10 m/s and the wind generator produces 2.84 kW. After 1.5 s the wind velocity decreases to 8 m/s and the wind conversion chain can deliver 1.45 kW. Finally, the wind speed changes to 5 m/s and the generated power is estimated to 350W as depicted in Fig 12(e).

The simulation model as presented in the Figure 13 (a) has adopted the generated random wind speed profile. The reference of the generator speed (wg_ref) varies according to the wind speed as depicted in Figure 13(b). The red rotational rotor speed is well monitored and controlled in response to the captured wind speed. Figure 13(c) indicates the profile of the generated inductor current and its reference; it is shown that the inductor current fluctuates around its desired value according of the wind speed variation. The Figure 13(d) depicts that the mechanical torque applied to PMSG generator reflects the same scenario for the variation of the meteorological conditions. The Figure 13(e) presents the simulation curve of the maximum wind power extracted from the wind turbine. An excellent and correct wind power trajectory is achieved accordingly as the wind velocity fluctuates.

C. Case 3: The grid side inverter response

This subsection presents the grid inverter performances by using the proposed MPC algorithm. Both active and reactive power exchanges between the three-phase inverter to the grid is given in Figure 14 (a, b). It can be seen that the injected active power (P_{active}) into the grid reflects the solar irradiance variation and the different wind speed levels. Once the solar irradiance is equal to 1000 W/m2 and the wind speed is estimated at 12 m/s, the PV-wind hybrid system provides a total active power, which is corresponding to its rated value (11.6 kW). When the climatic conditions change, the MPPT controller accurately extracts the maximum renewable power from the wind turbine and the PV generator. The Figure 14 is clearly indicates the difference between the generated power ($P_{turbine}$+P_{PV}) and the injected active power (P_{active}), which depends on the losses in different components of the power converter, including mainly power semi-conductor elements. Consequently, the injected active power is highly dependent on the wind speed profile and the solar variation with a response time equal to 0.06s. While the injected reactive power ($Q_{reactive}$) is kept at zero to maintain the unity power factor. As it is observed, in Figure 15 (a, b), the three-phase grid currents have sinusoidal waveforms according to the grid frequency (50Hz). The proposed MPC scheme indicates that the total harmonic distortion (THD) is about 0.95% for the grid current, which is very low as per IEEE 512-1992 standard. The grid-connected inverter controller keeps the DC-link voltage constant at 750V regardless of the wind velocity change. It reaches correctly its desired value over a set time period of 2s as presented in Figure 16 (a, b).In addition, it can be noted that the DC-bus voltage exhibits an almost negligible overshoot in transient response as well as in steady state (0.53%) with a settling time equal to 0.035s.

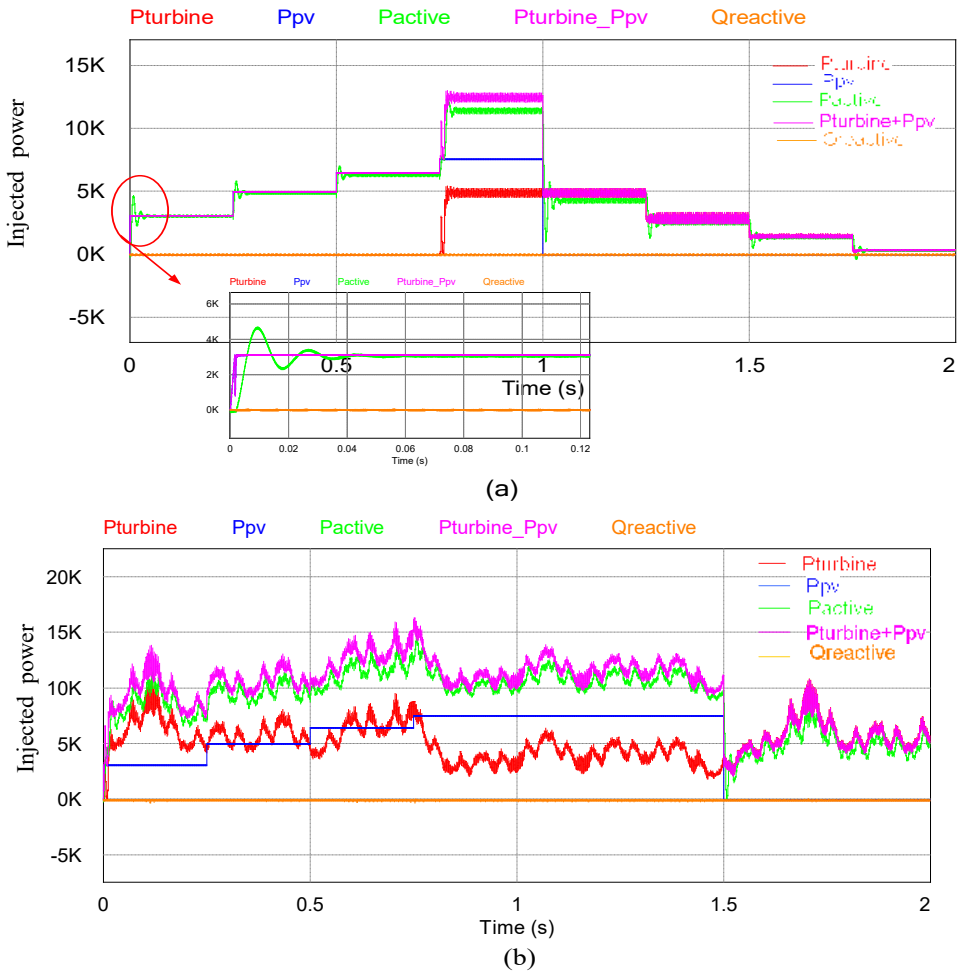

Figure 14. (a) Active and reactive under linear wind speed profile, (b) Active and reactive under random wind speed profile.

It is clearly visible, in the Figure 17 (a, b), that direct and quadrature current component respectively (igd and igq) evolve around their desired references with a reduced current ripple. Finally, the grid current and the main voltage are in phase as illustrated in Figure 18. The simulation results reveal that the developed model predictive control technique provides many advantages; A reduced fluctuation around maximum power point, an acceptable grid current THD compared to other conventional strategies reviewed in the literature, a pure sinusoidal current injected to the grid, an excellent tracking under divers operating weather conditions and good steady state performances. The proposed MPC algorithm is compared with the other previous studies in terms of settling time of PV power, settling time of rotor speed, settling time of DC-link voltage, response time of injected active power and Total Harmonic Distortion (THD) of the grid current. The comparison study with previous literature is mentioned in table 3.

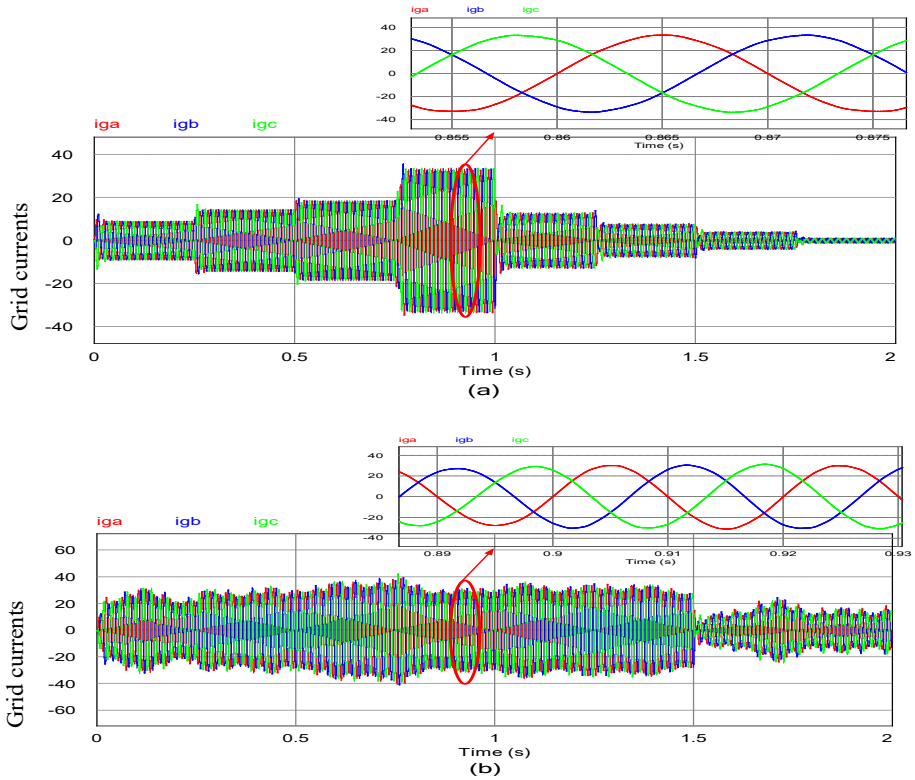

Figure 15. (a) Grid current waveforms under linear wind speed profile, (b) Grid current waveforms under random wind speed profile.

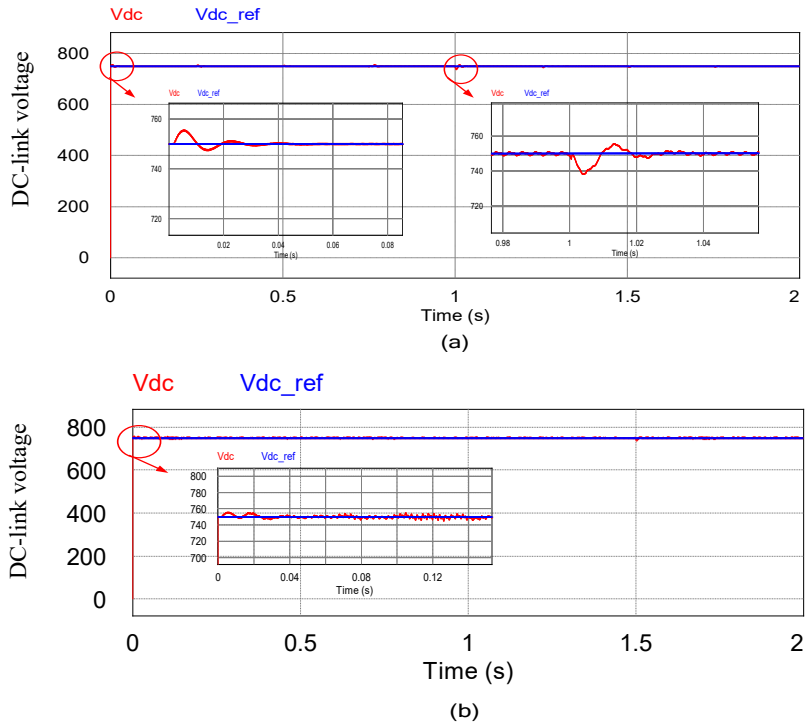

Figure 16. (a) DC-link voltage and its reference under linear wind speed profile, (b) DC-link voltage and its reference under random wind speed profile

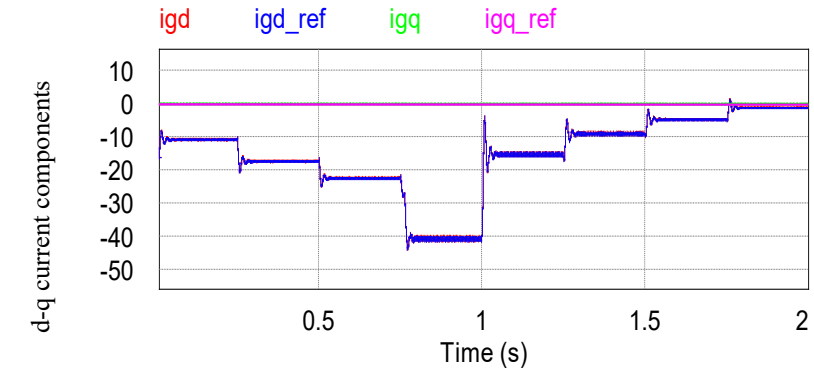

(a)

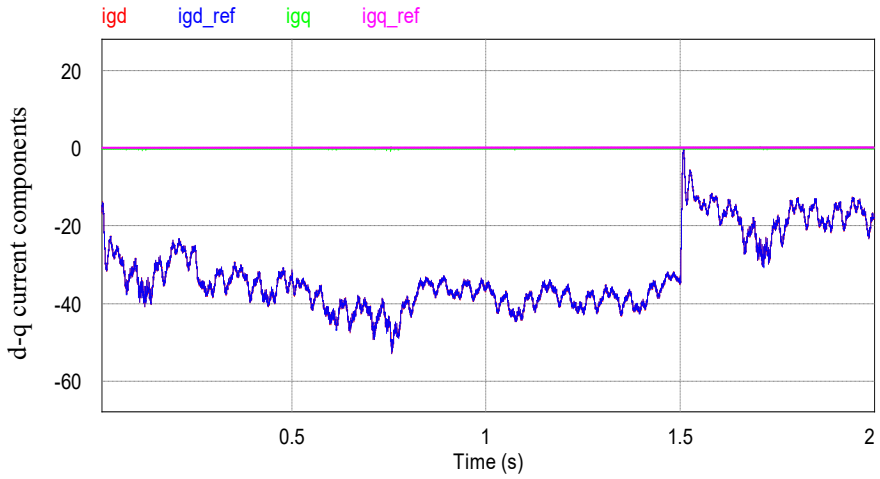

(b)

Figure 17. (a) qd-axis currents and their references under linear wind speed profile, (b) qd-axis currents and their references under random wind speed profile

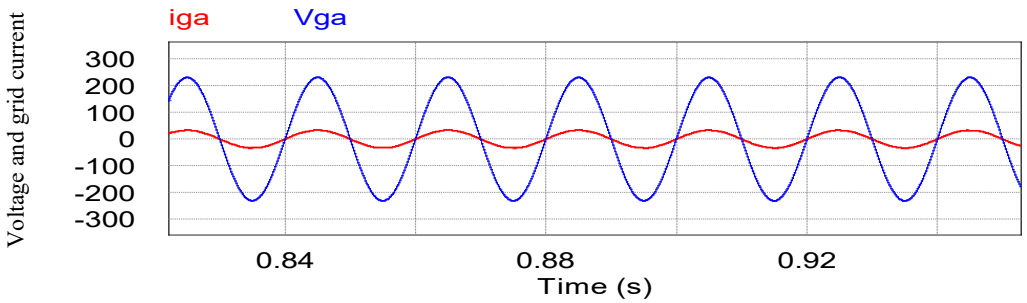

Figure 18. The grid current and the main voltage

Table 3. Comparison of the proposed MPC algorithm with ather existing method

Paper	Schemes	Control strategy	PV chain performance	Wind chain performance	Grid converter performance
[31]	Quasi-Z Source Inverter of PV Grid-connected	- a fuzzy proportional complex integral control	#	#	- THD: 1.36%
[32]	standalone solar-wind hybrid	intelligent Controller	- Settling time of PV power: 1.6s	#	- THD:1.83%
[33]	standalone hybrid PV-wind-battery system	(P&O) and PI controller	#	#	- THD: 1%
[34]	Grid-Connected PV system	- Practical Swarm Optimization (PSO) - Model predictive controller (FS-MPC)	- Settling time of PV power: 0.07s	#	- Settling time of DC-link voltage: 0.1s - Response time of active power: 0.13s - THD:0.66%
[35]	Hybrid system grid connected	Predictive Current Control	#	- Settling time of rotor speed: 0.1s	- THD:1.87%
The MPC algorithm	Grid Connected hybrid system	MPC strategy	- Settling time of PV power: 0.003s	- Settling time of rotor speed according wind speed (12m/s): 0.027s	- Settling time of DC-link voltage: 0.035s - Response time of active power: 0.06s - THD:0.95%

7. Conclusions

In this paper, a grid-connected hybrid energy system under solar and wind natural resources is properly designed. To validate the proposed control scheme performances under varying weather conditions, several computer simulations, using PSIM software, are carried out to verify the effectiveness of the adopted control technique. MPPT controller based on the MPC algorithm is applied for both photovoltaic and wind conversion chains. It has been tested under variable solar irradiance and wind velocity in order to track the maximum power from the renewable sources. The proposed MPC scheme for the grid-connected inverter has strongly enhanced the energy quality as per the standard in terms of a lower power fluctuation and reduced current THD.

8. References

[1]. Somudeep Bhattacharjee ; Champa Nandi ; Sushmita Reang , "Intelligent Energy Management Controller for Hybrid System, *3rd International Conference for Convergence in Technology (I2CT)*, 2018.

[2]. Tariq Kamal, Syed Zulqadar Hassan, Hui Li, Sidra Mumtaz, Laiq Khan "Energy Management and Control of Grid-Connected Wind/Fuel Cell/Battery Hybrid Renewable Energy System," *2016 International Conference on Intelligent Systems Engineering (ICISE)*, 15-17 Jan. 201615-17 Jan. 2016.

[3]. Tariq Kamal, Syed Zulqadar Hassan, "Energy Management and Simulation of Photovoltaic/Hydrogen/Battery Hybrid Power System," *Advances in Science, Technology and Engineering Systems Journal* Vol. 1, No. 2, 11-18, 2016.

[4]. Jayalakshmi N. S, D. N. Gaonkar,"Operation of Grid Integrated Wind/PV Hybrid System with Grid Perturbations," *International Journal of Renewable Energy Research*, Vol.5, No.4, 2015.

[5]. Hossam A. Gabbar, Mohamed El-Hendawi, G.El-Saady, El-Nobi A.Ibrahim, "Supervisory Controller for Power Management of AC/DC Microgrid," *the 4th IEEE International Conference on Smart Energy Grid Engineering*, 2016.

[6]. Mahsa Zarrini Farahmand, Mohammad Esmaeil Nazari, Sadegh Shamlou, "Optimal Sizing of an Autonomous Hybrid PV -Wind System Considering Battery and Diesel Generator," *25th Iranian Conference on Electrical Engineering (lCEE)*, 2017.

[7]. Dezso Sera, Laszlo Mathe, Tamas Kerekes, Sergiu Viorel Spataru, and Remus Teodorescu, On the Perturb-and-Observe and IncrementalConductance MPPT Methods for PV Systems, *IEEE JOURNAL OF PHOTOVOLTAICS*, VOL. 3, NO. 3, JULY 2013.

[8]. Nahla E. Zakzouk, Mohamed A. Elsaharty, Ahmed K. Abdelsalam, Ahmed A. Helal, Barry W. Williams, Improved performance low-cost incrementalconductance PV MPPT technique, IET Renewable Power Generation, 2015.

[9]. Karima Amara1, Toufik Bakir, Ali Malek, Dalila Hocine, El-Bay Bourennane, Arezki Fekik, and Mustapha Zaouia, «An Optimized Steepest Gradient Based Maximum Power Point Tracking for PV Control Systems », *International Journal on Electrical Engineering and Informatics*, volume 11, number 4, December 2019.

[10]. Mhamed Fannakh , Mohamed Larbi Elhafyani , Smail Zouggar Hardware implementation of the fuzzy logicMPPT in an Arduino card using a Simulinksupport package for PV application, IET Renewable Power Generation, November 2018.

[11]. Anang Tjahjono, Dimas Okky Anggriawan, Muhammad Nizar Habibi, and Eka Prasetyono, « Modified Grey Wolf Optimization for Maximum Power Point Tracking in Photovoltaic System under Partial Shading Conditions », *International Journal on Electrical Engineering and Informatics*, volume 12, number 1, March 2020.

[12]. Tao Zhao ; Qian Zong ; Tao Zhang ; You Xu , "Study of photovoltaic three-phase grid-connected inverter based on the grid voltage-oriented control," *11th Conference on Industrial Electronics and Applications (ICIEA)*, 2016.

[13]. Tao Zhao, Qian Zong, You Xu ,"Study of photovoltaic three-phase grid-connected inverter based on the grid voltage-oriented control," *IEEE 11th Conference on Industrial Electronics and Applications (ICIEA)*, 2016.

[14]. Ajesh P S1, Jisha Kuruvila P2, Dr. Anasraj R, "Analysis and Control of Three Phase PWM Rectifier for Power Factor Improvement of IM Drive," *International Journal of Innovations in Engineering and Technology (IJIET)*, 10 Issue 2 May2018.

[15]. Yonghao Gui, Gil Ha Lee, Chunghun Kim, Chung Choo Chung, "Direct power control of grid connected voltage source inverters using port-controlled Hamiltonian system," *International Journal of Control, Automation and Systems*, 2017.

[16]. T. A. Trivedi, R. Jadeja, P. Bhatt, "A Review on Direct Power Control for Applications to Grid Connected PWM Converters, " *Engineering, Technology & Applied Science Research* Vol. 5, No. 4, 2015, 841-849

[17]. D. Kalyanraj ; S. Lenin Prakash , "Design of sliding mode controller for three phase grid connected multilevel inverter for distributed generation systems," *21st Century Energy Needs-Materials, Systems and Applications (ICTFCEN)*, 2016.
[18]. Sid-Ahmed Touil ; Nasserdine Boudjerda ; Ahsene Boubakir ; Aimad Boudouda, "Sliding mode control of a grid-connected photovoltaic source via a three-phase inverter using incremental conductance MPPT," *5th International Conference on Electrical Engineering - Boumerdes (ICEE-B)*, 2017.
[19]. Ikram Maaoui-Ben Hassine, Mohamed Wissem Naouar, Najiba Mrabet-Bellaaj, "Model Based Predictive Control For Three-Phase Grid Connected Converter", *Journal electrical systems* 11-4 (2015):463-475
[20]. Irtaza M. Syed, Kaamran Raahemifar, "Model Predictive Control of Three Phase Inverter for PV Systems", World Academy of Science, Engineering and Technology International *Journal of Electrical, Computer, Energetic, Electronic and Communication Engineering* Vol:9, No:10, 2015
[21]. Qingzeng Yan, Xiaojie Wu, Xibo Yuan, Yiwen Geng, "An Improved Grid Voltage Feedforward Strategy for High-Power Three-Phase Grid-Connected Inverters Based on the Simplified Repetitive Predictor, " *IEEE transactions on power electronics*, volume 31, May 2016.
[22]. Arash Ahmadi, MohammadJavad Ahmadifar,Sobhan Ahmadi, "Three-Phase Inverter Control by Model Predictive Control, " *Research Journal of Recent Sciences*, ISSN 2277-2502, Vol. 4(1), 81-86, January (2015).
[23]. M.N. Amrani, A. Dib, "Predictive Direct Power Control of a Grid Connected Three-Phase Voltage Source Inverter for Photovoltaic Systems", *International Journal of Renewable Energy Research* Vol.6, No.1, 2016.
[24]. M. C. Cavalcanti, K. C. Oliveira, G. M. S. Azevedo, F. A. S. Neves, "Comarative study of Maximum Power Point Tracking Techniques For Photovoltaic Systems", Third *International Conference on Current Trends in Engineering Science and Technology ICCTEST*-2017.
[25]. Andres Larrea, Oscar Barambones, Jose A. Ramos-Herran, "Design and Implementation of a Predictive Control System for a Photovoltaic Generator", *IEEE 21st International Conference on Emerging Technologies and Factory Automation (ETFA).*
[26]. Omar Abdel-Rahim, Hirohito Funato, Junnosuke Haruna, "An efficient MPPT technique with fixed frequency finite-set model predictive control", *IEEE Energy Conversion Congress and Exposition (ECCE)*, 2015.
[27]. M. F. ELmorshedy ; S. M. Allam ; Essam M. Rashad , "Load voltage control and maximum power extraction of a stand-alone wind-driven PMSG including unbalanced operating conditions", *Eighteenth International Middle East Power Systems Conference (MEPCON),* 2016.
[28]. Seyed Mahyar Mehdizadeh moghadam, Esmail Alibeiki, and Alireza Khosravi, « Modelling And Control of 6MG Siemens Wind Turbine Blades Angle and Rotor Speed », *International Journal on Electrical Engineering and Informatics*, volume 11, number 1, March 2019.
[29]. M. Ruba, M. Babescu "Simulation analysis of a grid-connected wind energy conversion system", 10th *Jubilee International Symposium on Advanced Electromechanical Motion Systems* – Cluj-Napoca, Romania, 21-22 October 2013.
[30]. Bhadra R. Warrier, A. Vijayakumari and Sasi K. Kottayil, « Performance Evaluation of Model Predictive Current Controlled Grid Tied Converter for Sampling Frequency Variations », *International Journal on Electrical Engineering and Informatics*, volume 11, number 3, September 2019.
[31]. T. Hou, C.-Y. Zhang, H.-X. Niu "Quasi-Z Source Inverter Control of PV Gridconnected Based on Fuzzy PCI", *Journal of Electronic Science and Technology*, March 2020.

[32]. Partha Sarothi Sikder, Nitai Pal, "Modeling of an intelligent battery controller for standalone solar-windhybrid distributed generation system", *Journal of King Saud University – Engineering Sciences*, volume 32, issue 6, September 2020, pages 368-377.
[33]. Ayas Shaqour, Hooman Farzaneh, Yuichiro, Tatsuya Hinokuma, "Power control and simulation of a building integrated stand-alone hybrid PV-wind-battery system in Kasuga City, Japan" Energy Reports, volume 6, November 2020, pages 1528–1544.
[34]. Sami Meddoura, Djamel Rahema, Ali Yahia Cherifa, Walid Hachelfia, Laib Hichema, "A novel approach for PV system based on metaheuristic algorithm connected to the grid using FS-MPC controller", Energy Procedia volume 162, April 2019, pages 57-66.
[35]. Ridha BENADU, Brahim KHIARI, Anis SELLAMI, "Predictive Current Control Strategy for a Three-Phase Grid Connected PhotovoltaicWind Hybrid System", *7th International Renewable Energy Congress (IREC)*, March 2016.

Houda LAABIDI was born in El Kef, Tunisia, on February 21, 1986. She received the Mastery degree in Electrical Engineering from the Higher School of Technology and Computer Science (ESTI), Tunis, Tunisia, in 2009, and the master s degree in Electrical Engineering from the National Engineering School of Tunis (ENIT), Tunis, Tunisia, in 2011. Since 2012, she has been a teacher at ESPRIT School of Engineering. She is currently working toward the PhD in Laboratoire d'Application de l'Efficacité Energétique et des Energies Renouvelables, LAPER, FST. Her research interests are in the photovoltaic-wind hybrid system connected to micogrid.

Houda Jouini was born in Tunisia, She received the Ing. and M.S. degrees in Industrial computing from Carthage University- National Institute of Applied Sciences and Technologies, INSAT. She received the PHD degree in 2011 from Tunis University- Higher School of Science and Technology of Tunis, ESSTT. She is currently an Associate Professor in the Physic Department at the Faculty of science of Tunis, Tunisia, University Tunis El Manar and a scientific researcher in energy applications and renewable energy efficiency Laboratory (LAPER). Her research interests include renewable energy system connected to micro-grid and power quality improvement.

Abdelkader Mami is a Tunisian Professor, in the University EI Manar at the Faculte des Sciences de Tunis. He received his Diploma of Electrical Engineering from the Tunisian University; His had his PHD of Science in Control Engineering from Aix Marseille University in France, and became Associate Professor in France at Lille University in 2003.